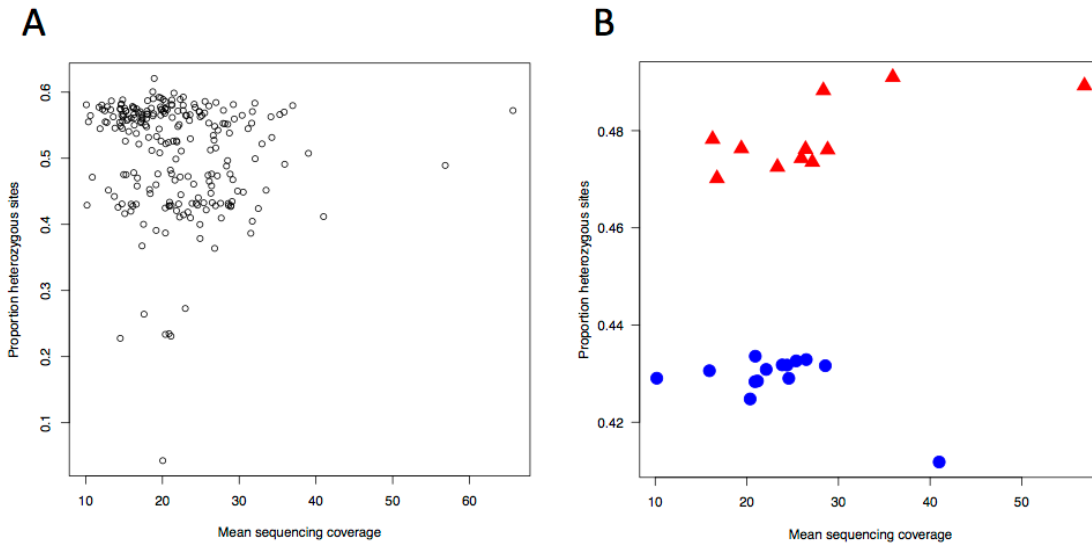
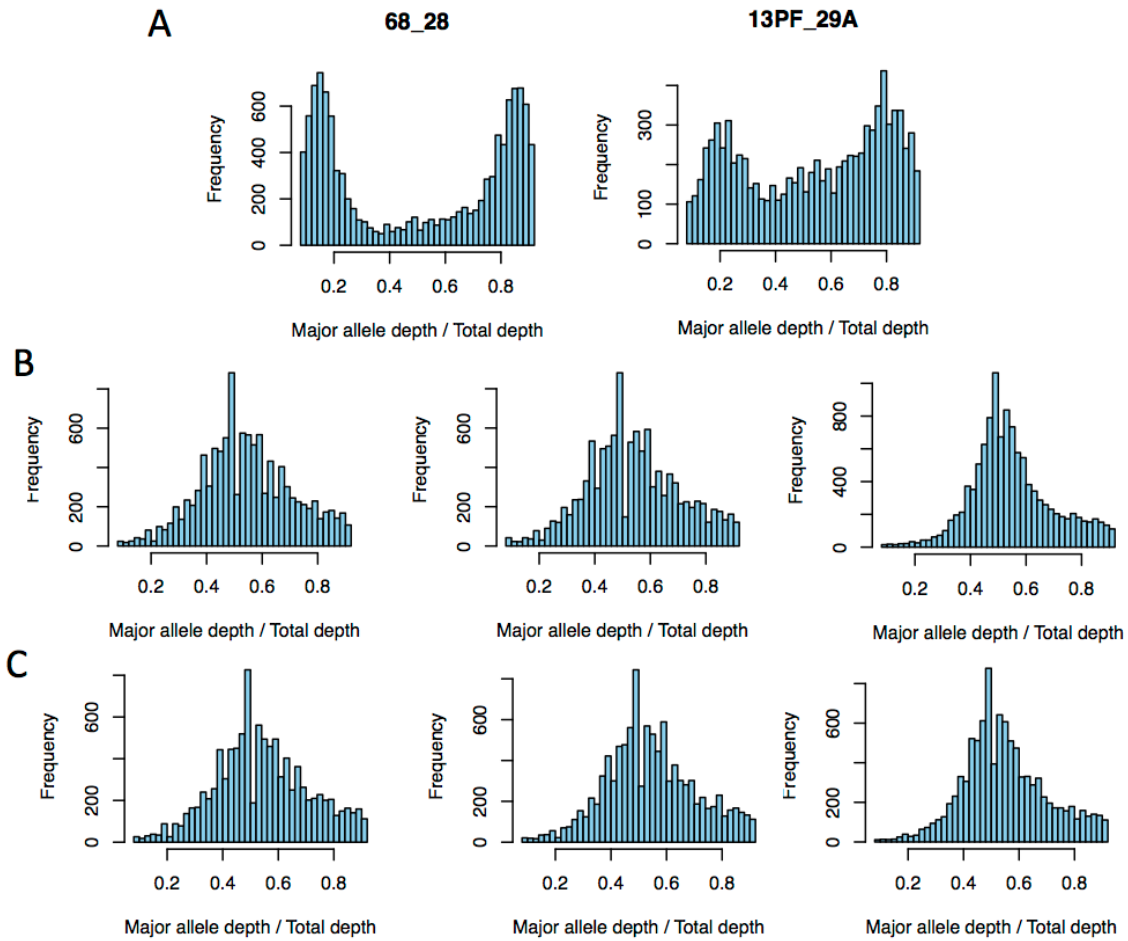


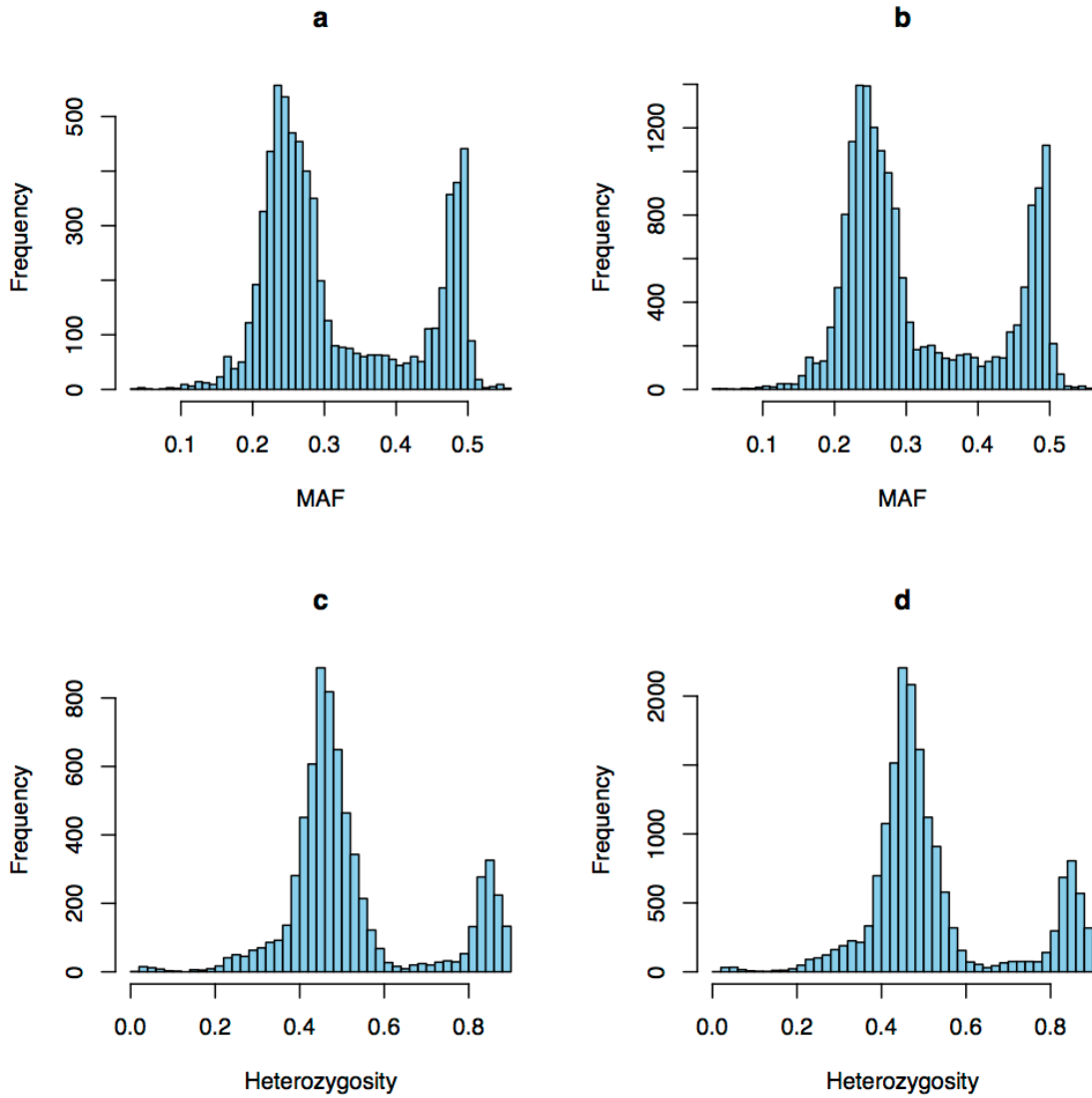
**Figure S1. SNP and individual filtering pipeline.** Gray and white shaded boxes indicate SNP filtering steps. Orange shaded boxes indicate individual filtering steps.



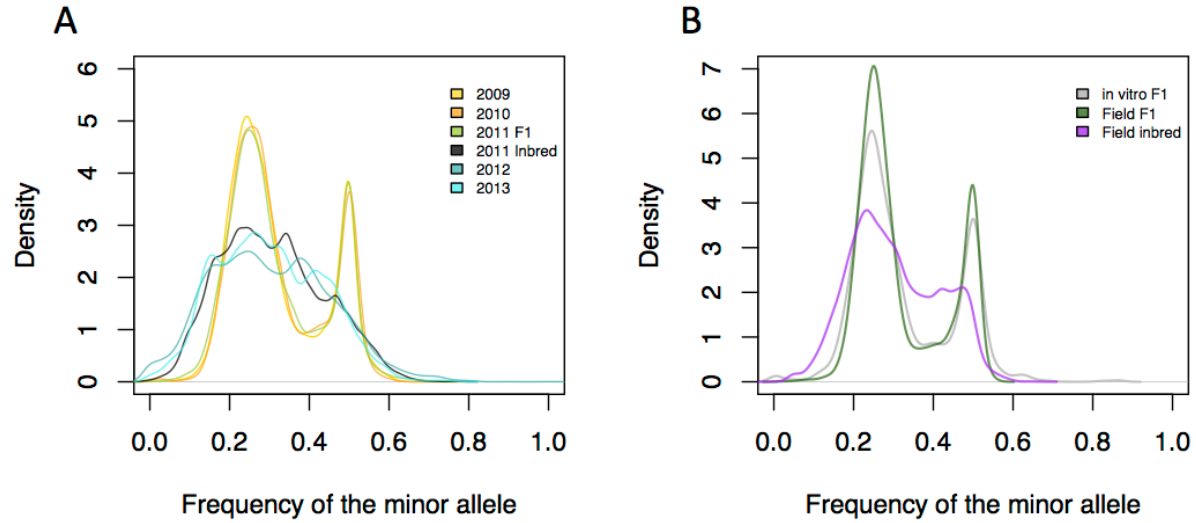
**Figure S2. Relationship between sequencing coverage and heterozygosity.** The proportion of heterozygous genotypes per sample plotted against individual mean sequencing coverage ( $n=23,485$  SNPs). A) For all samples prior to clone-correction and outlier removal, and B) for only replicates of the A1 parental isolate ( $n=14$ ; blue circles) and the A2 parental isolate ( $n=11$ ; red triangles).



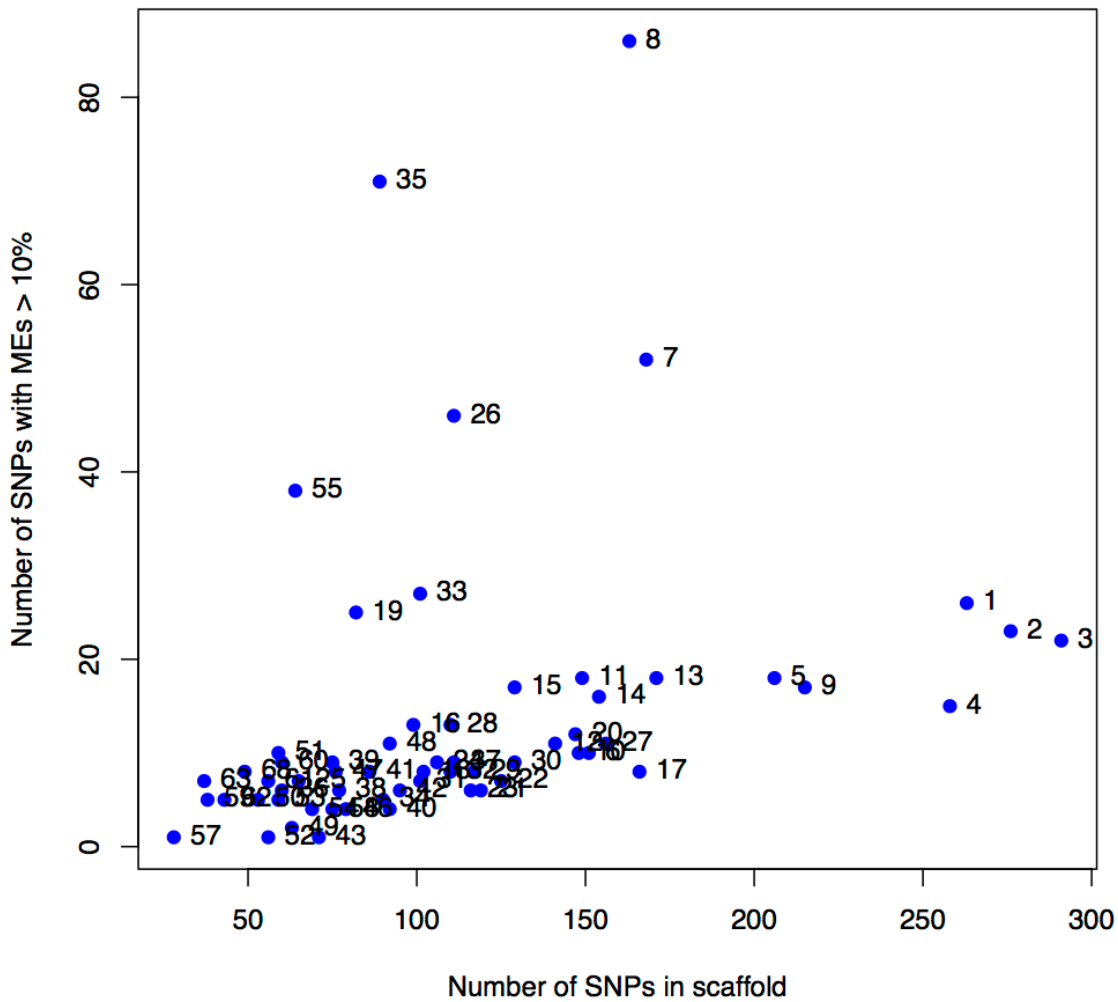
**Figure S3. Skewed allele depth ratios in two isolates suggest ploidy variation.** Histograms of the ratio of the major allele depth to the total depth for each heterozygous genotype for each isolate (at 23,485 SNPs). A) One *in vitro* and one field isolate display grossly aberrant allele depth ratios suggestive of ploidy variation. In contrast, allele depth ratios for the (B) A1 and (C) A2 parental isolates were centered at approximately 0.5.



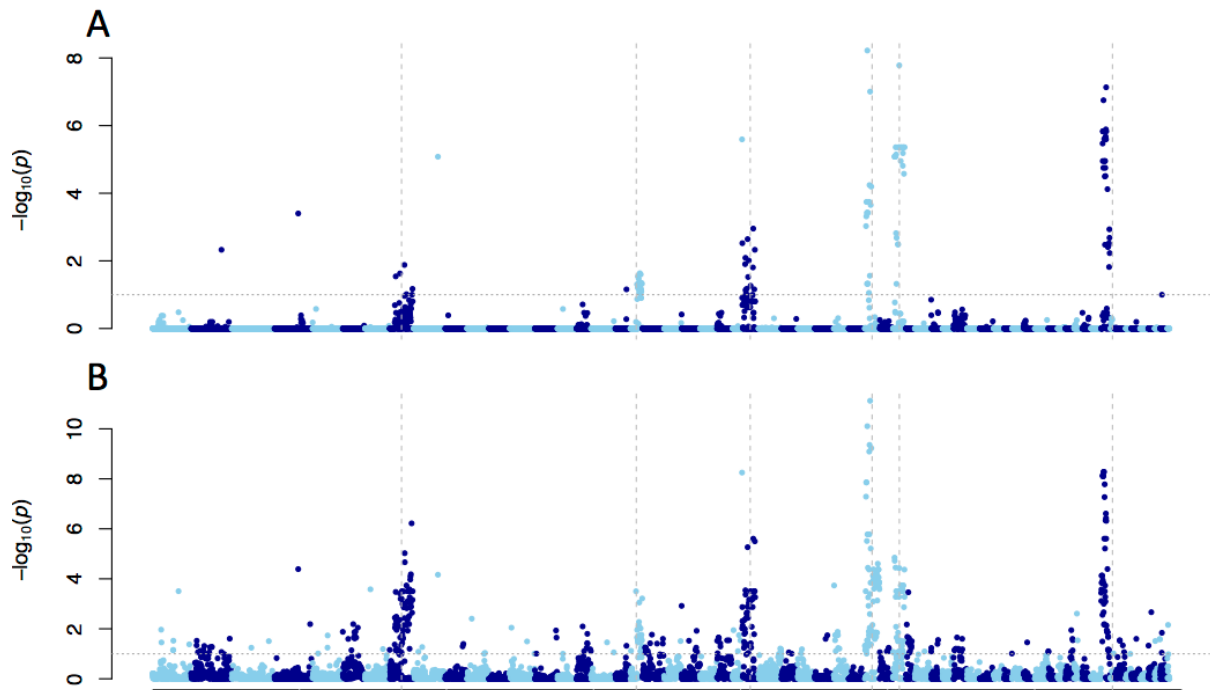
**Figure S4. Comparing pruned and unpruned data sets.** Minor allele frequency (MAF) and heterozygosity distributions for the unpruned ( $n=17,267$ ) and pruned SNPs ( $n=6,916$ ) in the field population ( $n=159$  isolates). (A) and (C) are for the pruned data set. (B) and (D) are for the unpruned data set.



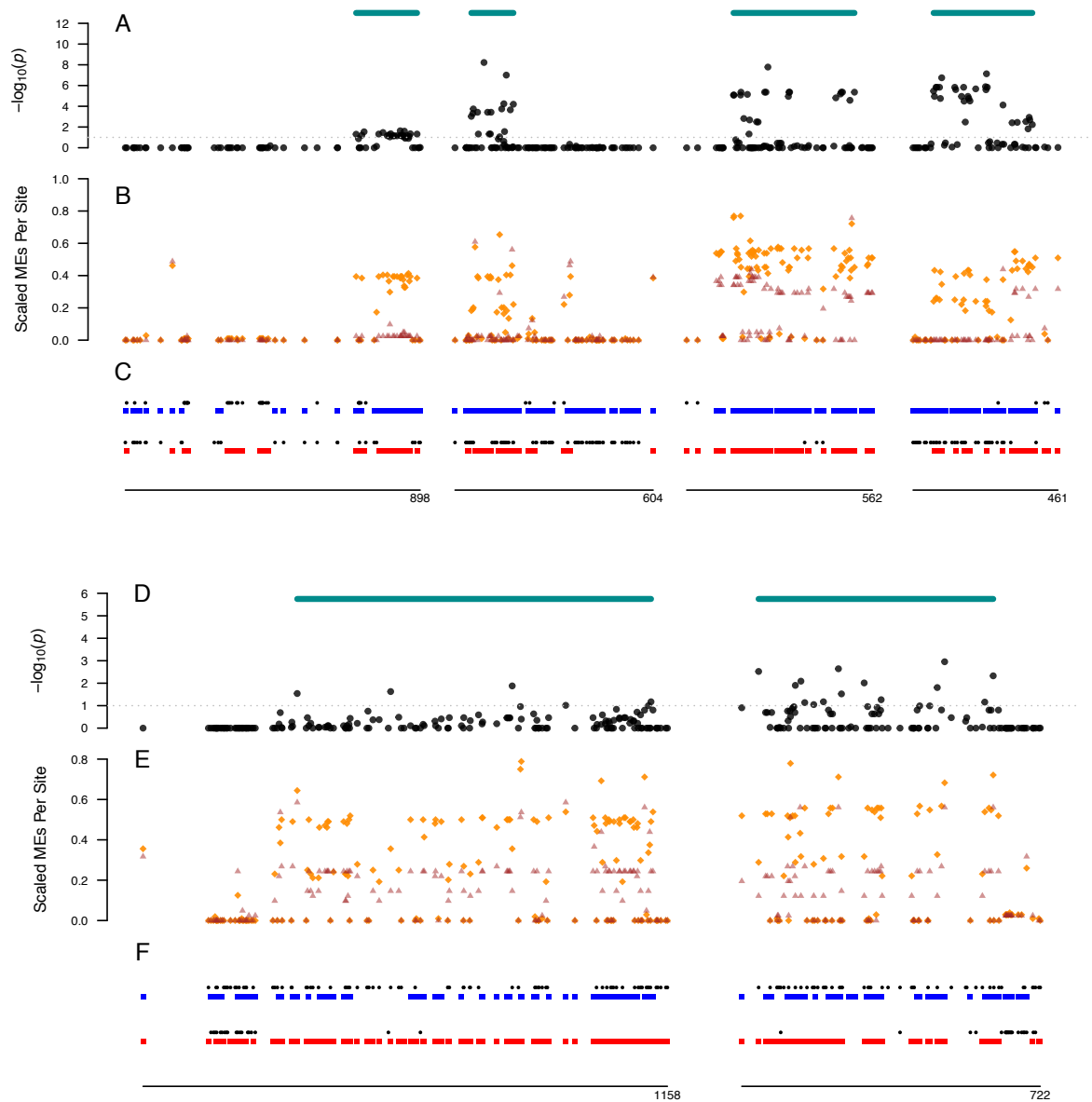
**Figure S5. Minor allele frequency (MAF) distributions for the field and *in vitro* populations.** A) MAF distributions for each year in the field population. Year 2011 was split into F<sub>1</sub> and inbred isolates based on classification via Mendelian errors, showing that the 2011 F<sub>1</sub> contingent MAF distribution was similar to that of 2009 and 2010, which contained exclusively F<sub>1</sub> isolates. Within years containing F<sub>1</sub> isolates, we observe peaks at 0.25 and 0.5, consistent with expectations for a population derived from only two parents. B) The field F<sub>1</sub> subpopulation MAF distribution was consistent with the that of the *in vitro* F<sub>1</sub>. The field Inbred MAF distribution deviated from expectations for an F<sub>1</sub>, denoting allele frequency changes.



**Figure S6. Relationship between number of SNPs in each scaffold and the incidence of Mendelian error (ME) enriched SNPs among the *in vitro* F<sub>1</sub> and empirically defined field F<sub>1</sub> ( $n=143$ ) prior to removal of the ME enriched SNPs.** SNPs enriched for MEs were defined as SNPs where greater than 10% of *in vitro* F<sub>1</sub> and field F<sub>1</sub> isolates had a ME (at least 15 isolates). The number of ME enriched SNPs was plotted as a function of the number of SNPs in each scaffold, identifying seven scaffolds (7, 8, 19, 26, 33, 35, and 55) with excess ME-enriched SNPs relative to the other scaffolds. Data points are labeled with the scaffold number.

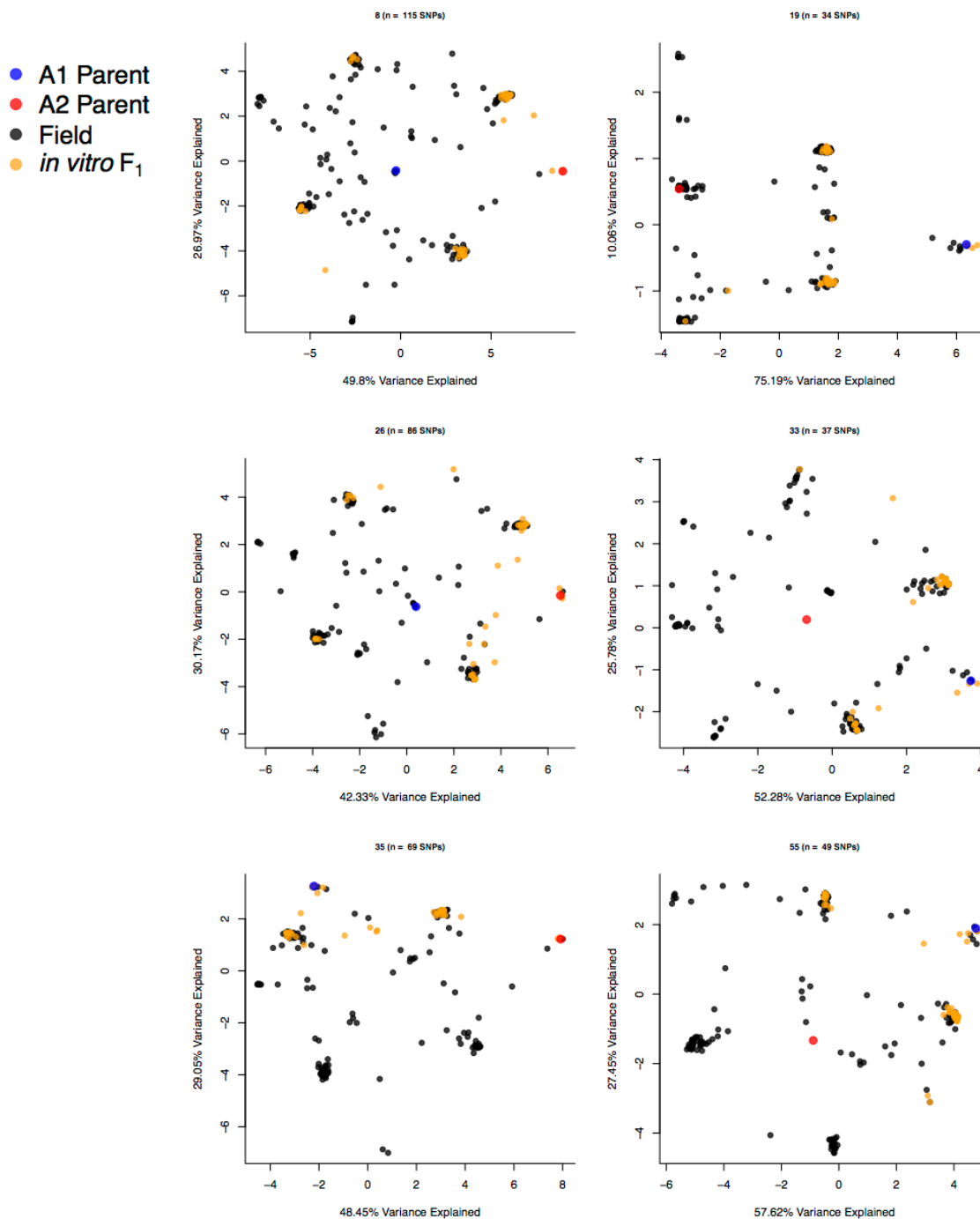


**Figure S7. Regions of differentiation between the *in vitro* F<sub>1</sub> and the field F<sub>1</sub> and field inbred subpopulations identified using Fisher's exact tests of allele frequency differences at each SNP.** Negative log<sub>10</sub>-transformed, false-discovery rate (FDR) adjusted, *P*-values from pairwise comparisons between the (A) *in vitro* F<sub>1</sub> and field F<sub>1</sub> and (B) *in vitro* F<sub>1</sub> and field inbred plotted for each SNP. SNPs are ordered relative to physical position and colors alternate by scaffold. Gray vertical dashed lines in A-C indicate scaffolds pertaining to regions of differentiation between the *in vitro* F<sub>1</sub> and the field F<sub>1</sub>. The gray dotted line in A and B denotes the 10% FDR threshold.



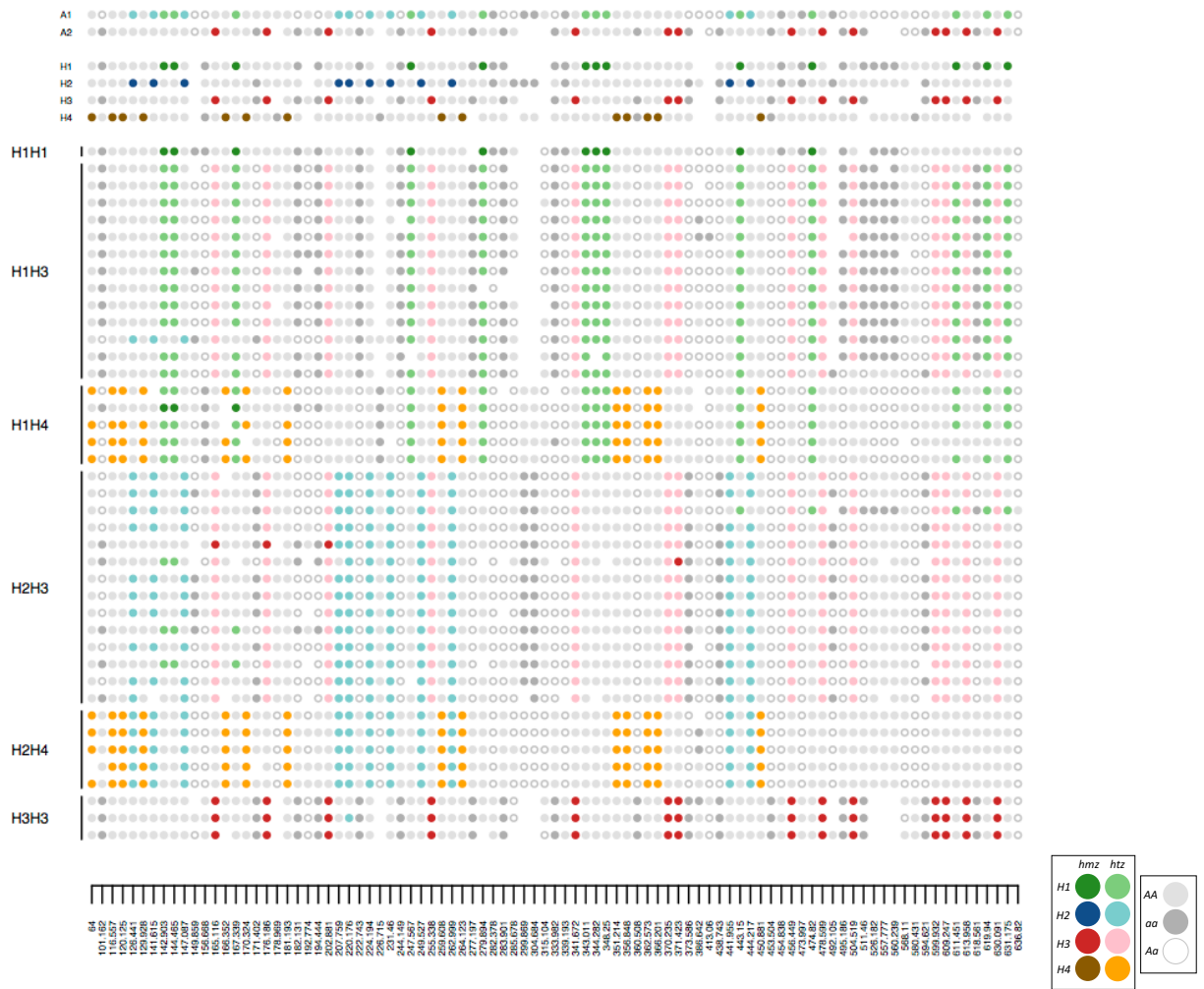
**Figure S8. Regions of differentiation between the *in vitro* F<sub>1</sub> and field F<sub>1</sub> were associated with loss of heterozygosity (LOH) events in the parental cultures.** A) and D) show the negative log<sub>10</sub>-transformed, FDR adjusted, *P*-values from the Fisher's exact test of allele frequency differences between the *in vitro* F<sub>1</sub> and field F<sub>1</sub>, relative to physical position (kb), in scaffolds corresponding regions of differentiation. The teal bars span each differentiated region. B) and E) show the proportion of individuals with a Mendelian error (ME) for each SNP in the *in vitro* F<sub>1</sub> (brown triangles) and the field F<sub>1</sub> (orange diamonds), excluding homozygous isolates. C) and F) are the parental genotypes represented by blue (A1 parent) and red (A2 parent) squares for homozygous genotypes and black dots for heterozygous genotypes. A-C show, in order, scaffolds 19, 33, 35, and 55. And, D-F show, in order, scaffolds 8 and 26.

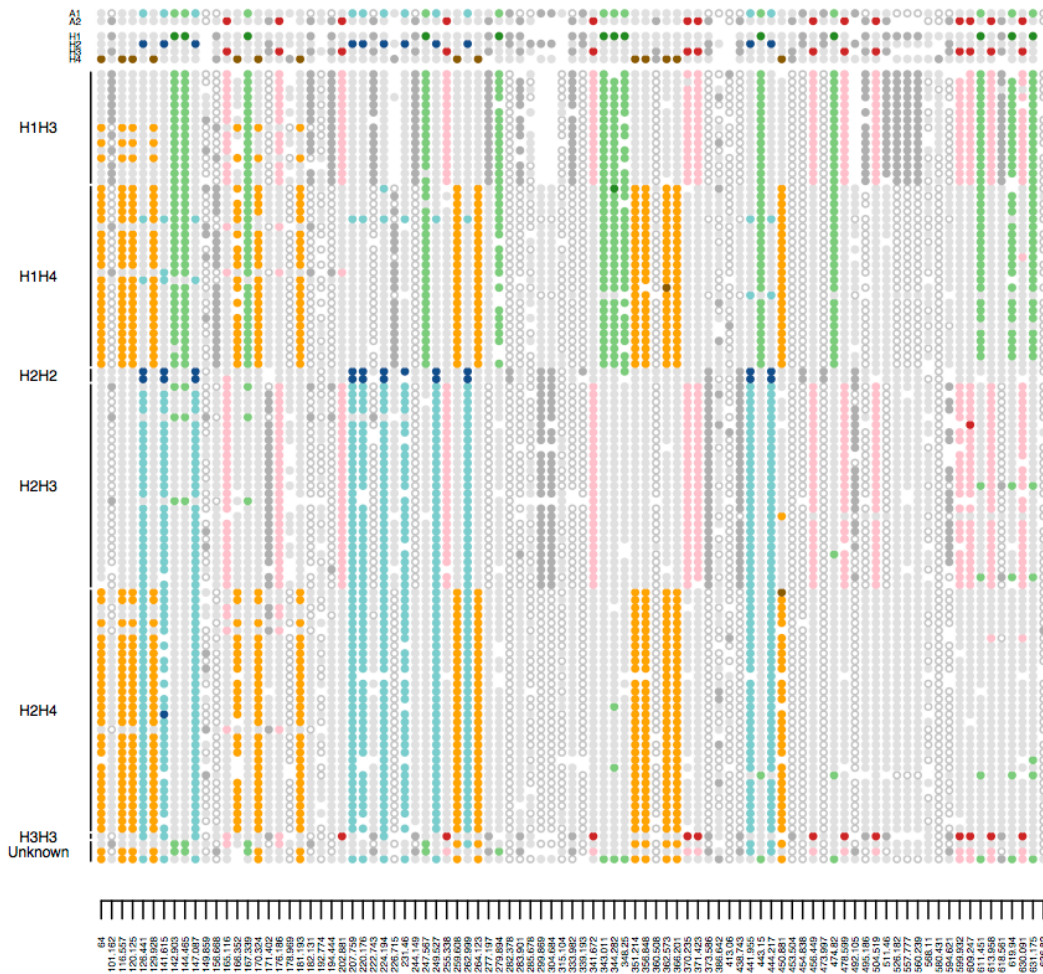




**Figure S9. Principal component analysis (PCA) in scaffolds pertaining to regions of interest (ROIs).** PCA was performed on the *in vitro* F<sub>1</sub>, field F<sub>1</sub>, and the field inbred isolates, as well as, the consensus parental genotypes with only SNPs in each of the six differentiated regions. All PCAs show four primary clusters, corresponding to four genotypic classes. The field isolates ( $n=159$ ) are represented by closed, black circles. The *in vitro* F<sub>1</sub> ( $n=41$ ) are represented by orange, closed circles. The A1 and A2 consensus parental genotypes are represented by blue and red closed circles, respectively.

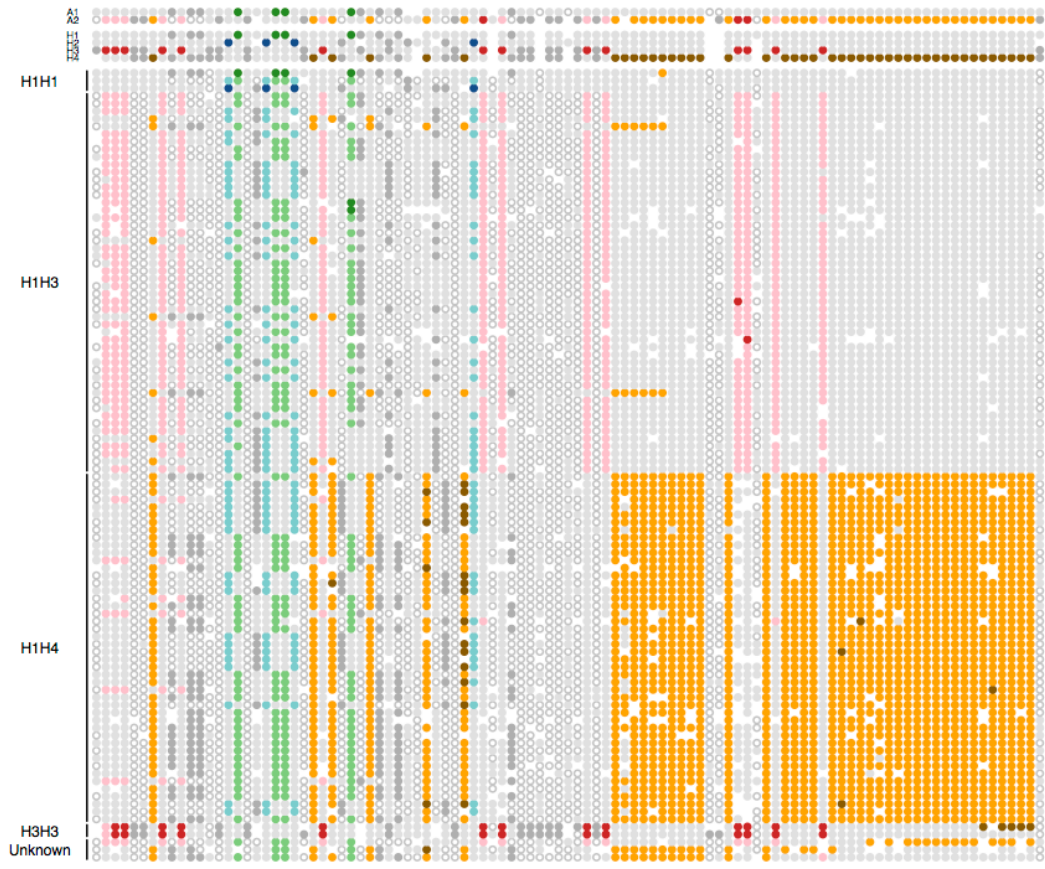
A



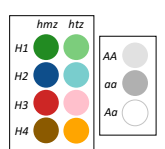
**B**

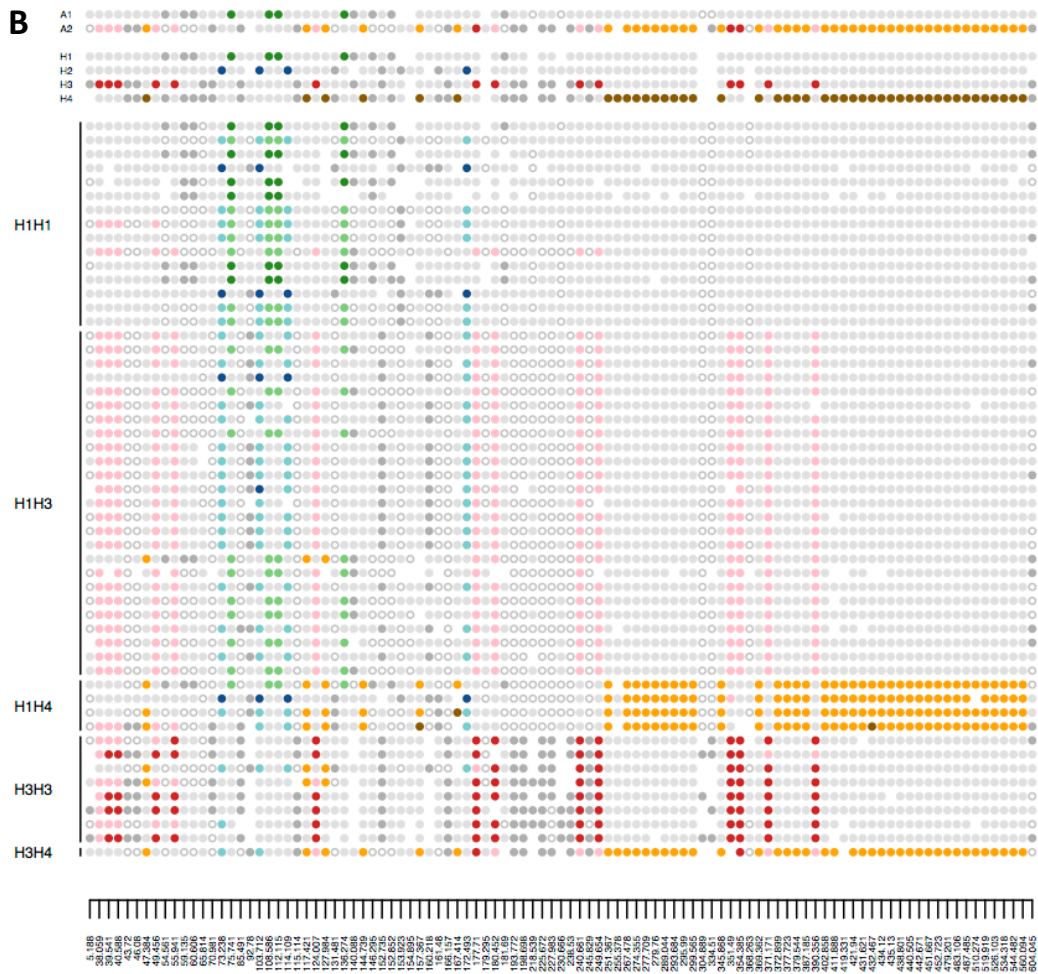
**Figure S10. Phase diagram for R-26 (scaffold 26).** Haplotype tagging SNPs were identified from the phased parental genotypes, and each isolate genotype was represented with respect to these tagging SNPs (see Methods). Closed, colored circles indicate haplotype tagging SNPs, with darker colors indicating the homozygote state, and lighter shades indicating the heterozygous state. Filled, gray circles indicate homozygous genotypes at non-tagging SNPs, whereas open, gray circles indicate heterozygous genotypes at non-tagging SNPs (see legend). Missing genotypes are denoted by the absence of a circle. Phase diagrams for the parental isolates (top), identified haplotypes (middle) and (A) *in vitro* F<sub>1</sub> and (B) field F<sub>1</sub>.

A



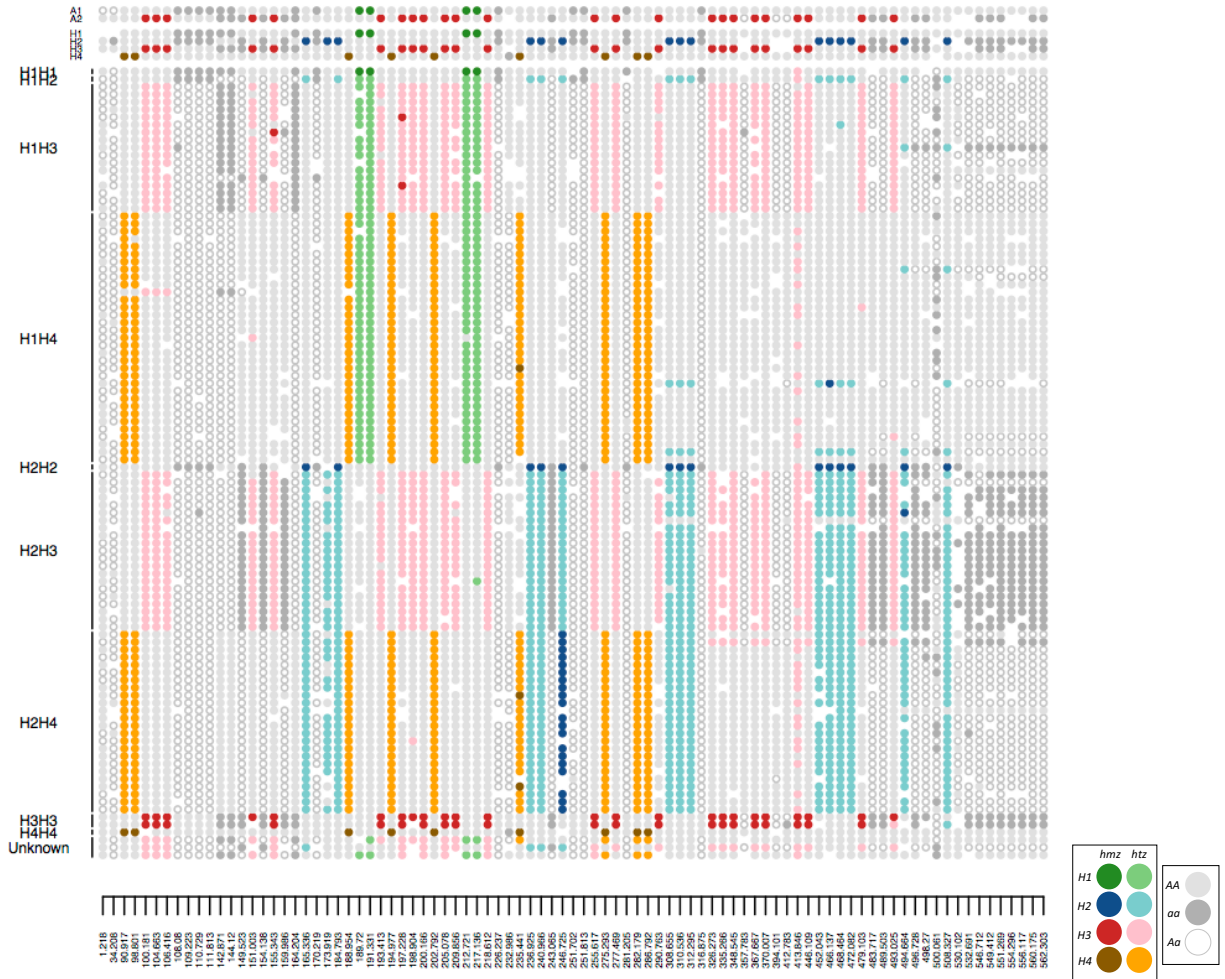
38 39 40 41 42 43 44 45 46 47 48 49 50 51 52 53 54 55 56 57 58 59 60 61 62 63 64 65 66 67 68 69 70 71 72 73 74 75 76 77 78 79 80 81 82 83 84 85 86 87 88 89 90 91 92 93 94 95 96 97 98 99 100 101 102 103 104 105 106 107 108 109 110 111 112 113 114 115 116 117 118 119 120 121 122 123 124 125 126 127 128 129 130 131 132 133 134 135 136 137 138 139 140 141 142 143 144 145 146 147 148 149 150 151 152 153 154 155 156 157 158 159 160 161 162 163 164 165 166 167 168 169 170 171 172 173 174 175 176 177 178 179 180 181 182 183 184 185 186 187 188 189 190 191 192 193 194 195 196 197 198 199 200 201 202 203 204 205 206 207 208 209 210 211 212 213 214 215 216 217 218 219 220 221 222 223 224 225 226 227 228 229 230 231 232 233 234 235 236 237 238 239 240 241 242 243 244 245 246 247 248 249 250 251 252 253 254 255 256 257 258 259 260 261 262 263 264 265 266 267 268 269 270 271 272 273 274 275 276 277 278 279 280 281 282 283 284 285 286 287 288 289 290 291 292 293 294 295 296 297 298 299 300 301 302 303 304 305 306 307 308 309 310 311 312 313 314 315 316 317 318 319 320 321 322 323 324 325 326 327 328 329 330 331 332 333 334 335 336 337 338 339 340 341 342 343 344 345 346 347 348 349 350 351 352 353 354 355 356 357 358 359 360 361 362 363 364 365 366 367 368 369 370 371 372 373 374 375 376 377 378 379 380 381 382 383 384 385 386 387 388 389 390 391 392 393 394 395 396 397 398 399 400 401 402 403 404 405 406 407 408 409 410 411 412 413 414 415 416 417 418 419 420 421 422 423 424 425 426 427 428 429 430 431 432 433 434 435 436 437 438 439 440 441 442 443 444 445 446 447 448 449 450 451 452 453 454 455 456 457 458 459 460 461 462 463 464 465 466 467 468 469 470 471 472 473 474 475 476 477 478 479 480 481 482 483 484 485 486 487 488 489 490 491 492 493 494 495 496 497 498 499 500 501 502 503 504 505 506 507 508 509 510 511 512 513 514 515 516 517 518 519 520 521 522 523 524 525 526 527 528 529 530 531 532 533 534 535 536 537 538 539 540 541 542 543 544 545 546 547 548 549 550 551 552 553 554 555 556 557 558 559 560 561 562 563 564 565 566 567 568 569 570 571 572 573 574 575 576 577 578 579 580 581 582 583 584 585 586 587 588 589 590 591 592 593 594 595 596 597 598 599 600 601 602 603 604 605 606 607 608 609 610 611 612 613 614 615 616 617 618 619 620 621 622 623 624 625 626 627 628 629 630 631 632 633 634 635 636 637 638 639 640 641 642 643 644 645 646 647 648 649 650 651 652 653 654 655 656 657 658 659 660 661 662 663 664 665 666 667 668 669 670 671 672 673 674 675 676 677 678 679 680 681 682 683 684 685 686 687 688 689 690 691 692 693 694 695 696 697 698 699 700 701 702 703 704 705 706 707 708 709 710 711 712 713 714 715 716 717 718 719 720 721 722 723 724 725 726 727 728 729 730 731 732 733 734 735 736 737 738 739 740 741 742 743 744 745 746 747 748 749 750 751 752 753 754 755 756 757 758 759 760 761 762 763 764 765 766 767 768 769 770 771 772 773 774 775 776 777 778 779 780 781 782 783 784 785 786 787 788 789 790 791 792 793 794 795 796 797 798 799 800 801 802 803 804 805 806 807 808 809 810 811 812 813 814 815 816 817 818 819 820 821 822 823 824 825 826 827 828 829 830 831 832 833 834 835 836 837 838 839 840 841 842 843 844 845 846 847 848 849 850 851 852 853 854 855 856 857 858 859 860 861 862 863 864 865 866 867 868 869 870 871 872 873 874 875 876 877 878 879 880 881 882 883 884 885 886 887 888 889 890 891 892 893 894 895 896 897 898 899 900 901 902 903 904 905 906 907 908 909 910 911 912 913 914 915 916 917 918 919 920 921 922 923 924 925 926 927 928 929 930 931 932 933 934 935 936 937 938 939 940 941 942 943 944 945 946 947 948 949 950 951 952 953 954 955 956 957 958 959 960 961 962 963 964 965 966 967 968 969 970 971 972 973 974 975 976 977 978 979 980 981 982 983 984 985 986 987 988 989 990 991 992 993 994 995 996 997 998 999 1000

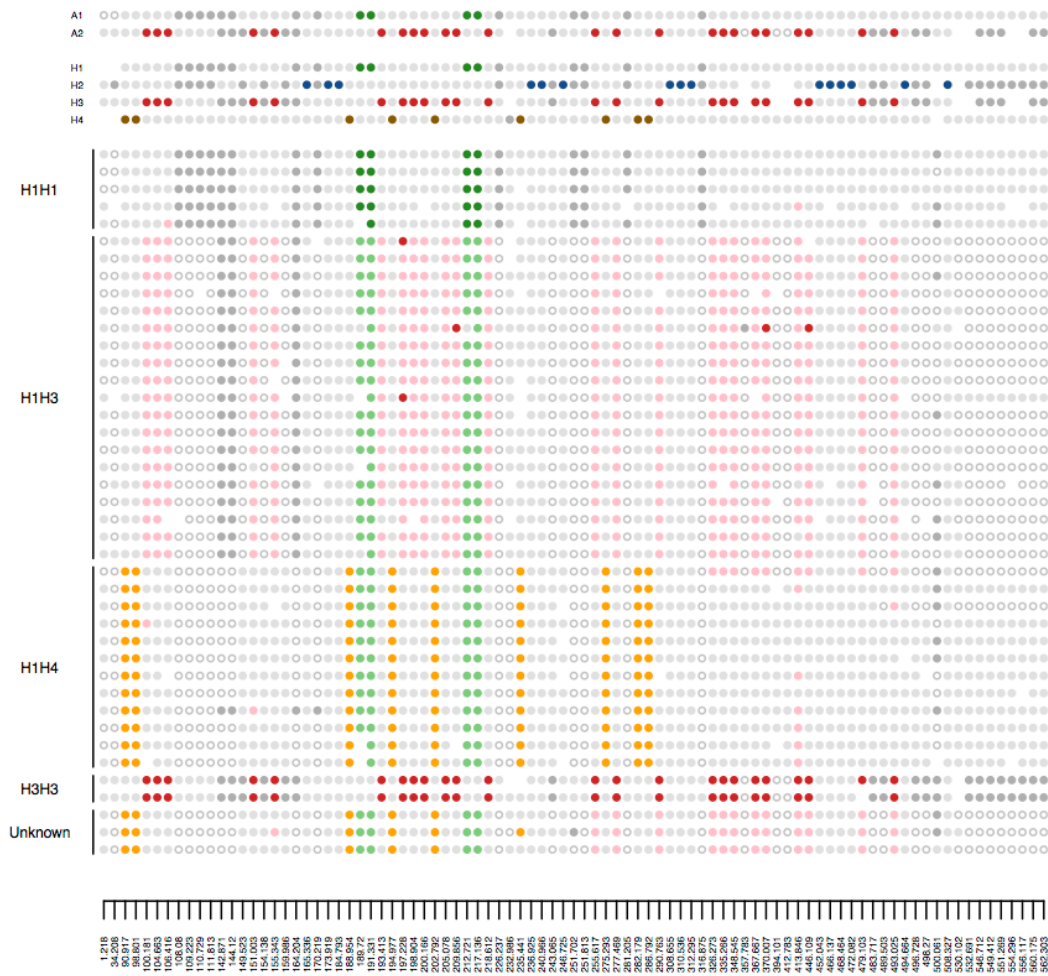




**Figure S11. Phase diagram for ROI-1 (scaffold 33).** Labeled genotypes based on ROI-1 only. Haplotype tagging SNPs were identified from the phased parental genotypes, and each isolate genotype was characterized with respect to the tagging SNPs (see Methods). Closed, colored circles indicate haplotype tagging SNPs, with darker colors indicating the homozygote state, and lighter shades indicating the heterozygous state. Filled, gray circles indicate homozygous, non-tagging genotypes, whereas open, gray circles indicate heterozygous non-tagging genotypes (see legend). Missing genotypes are denoted by the absence of a circle. Phase diagrams for the parental isolates (top), identified haplotypes (middle) and (A) field F<sub>1</sub> and (B) field inbred (bottom).

A



**B**

**Figure S12. Phase diagram for R-35 (scaffold 35).** Haplotype tagging SNPs were identified from the phased parental genotypes, and each isolate genotype was characterized with respect to the tagging SNPs (see Methods). Closed, colored circles indicate haplotype tagging SNPs, with darker colors indicating the homozygote state, and lighter shades indicating the heterozygous state. Filled, gray circles indicate homozygous, non-tagging genotypes, whereas open, gray circles indicate heterozygous non-tagging genotypes (see legend). Missing genotypes are denoted by the absence of a circle. Phase diagrams for the parental isolates (top), identified haplotypes (middle) and (A) field F<sub>1</sub> and (B) *in vitro* F<sub>1</sub>.

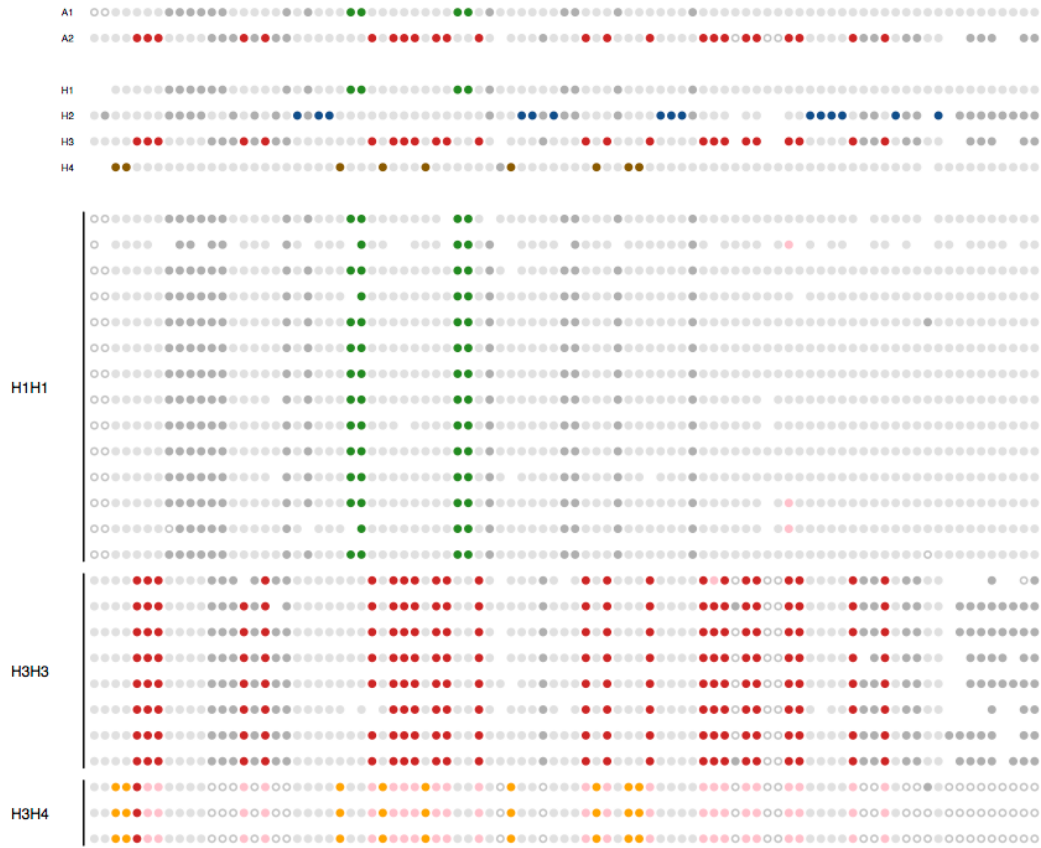


**Figure S13. Phase diagrams for the parental replicates in R-35 (scaffold 35).** All A1 parental replicates were H1/H1. The three A2 parental replicates sequenced prior to 2014 were H3/H4, whereas the later sequenced replicates were H3/H3 (see S1 Table).



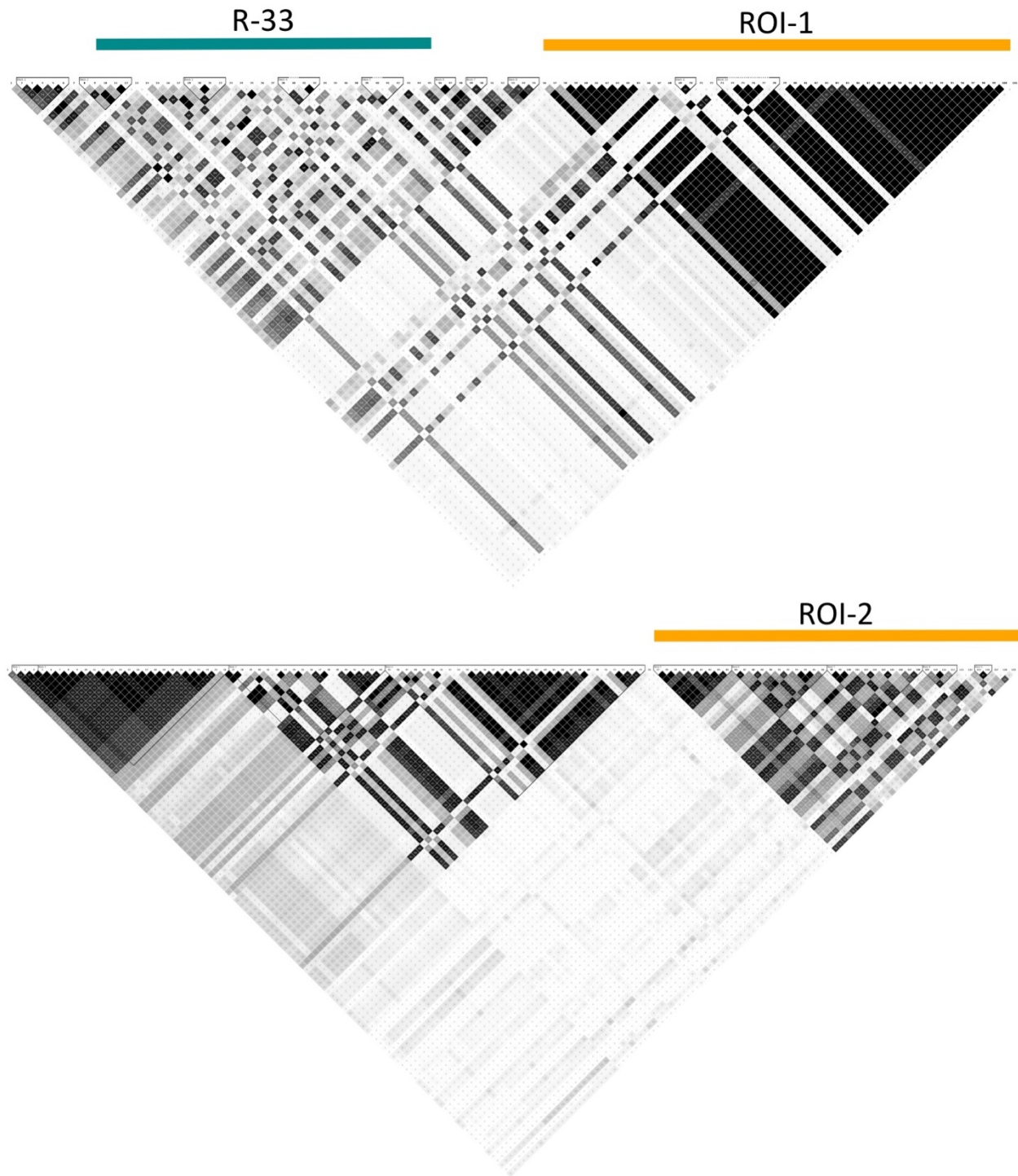


**Figure S14. Linkage disequilibrium (LD) in regions of interest (ROIs).** ROIs are indicated by orange bars. A) LD in scaffold 33 which contains both R-33 (denoted by a teal bar) and ROI-1. B) LD in scaffold 26, which contains ROI-2.

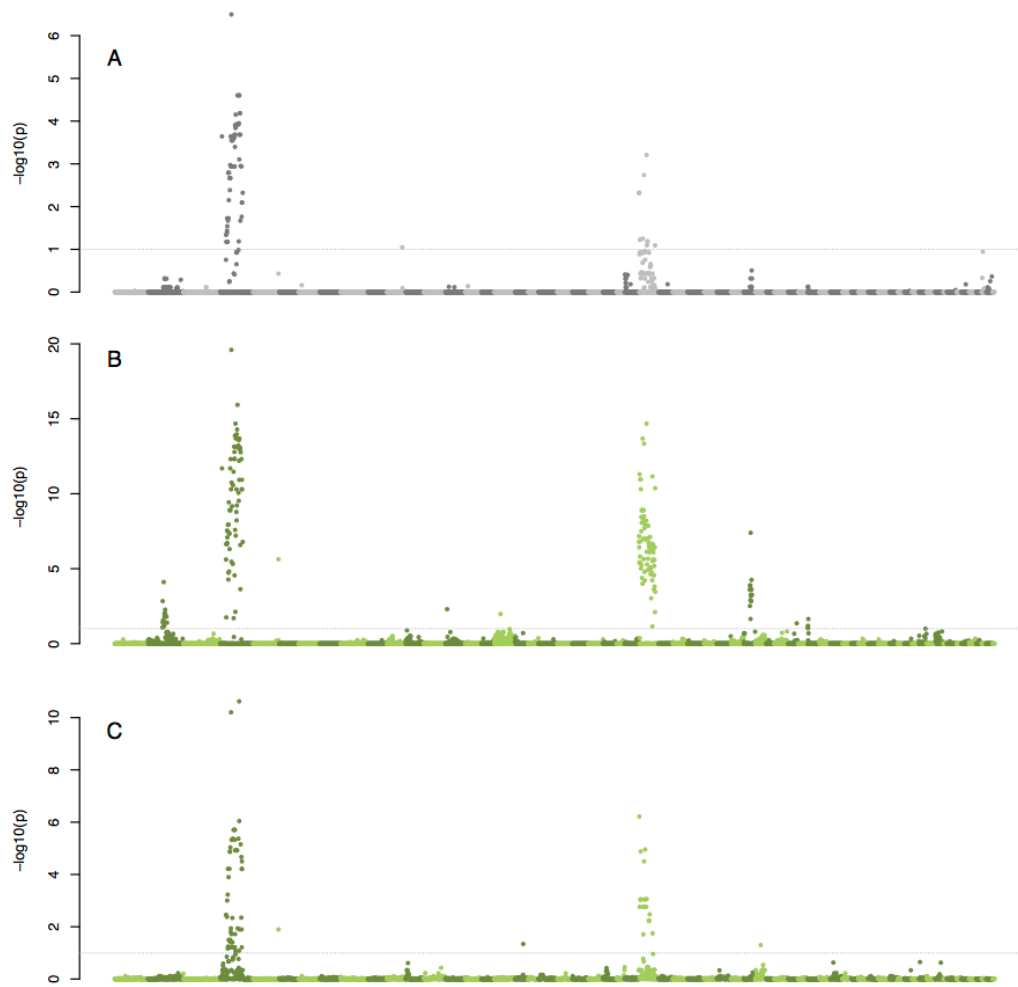


**Figure S15. Allele frequency differences between isolates of opposite mating types in the *in vitro* F<sub>1</sub>, field F<sub>1</sub>, and field inbred subpopulations.** Negative log<sub>10</sub>-transformed, FDR corrected *P*-values ordered by scaffold and physical position, from the Fisher's exact test of allele frequency differences between A1 and A2 isolates in the (A) *in vitro* F<sub>1</sub>, (B) field F<sub>1</sub>, and (C) field inbred subpopulations. SNPs above the gray lines in A-C were significant at a 10% false-discovery rate (FDR) threshold.

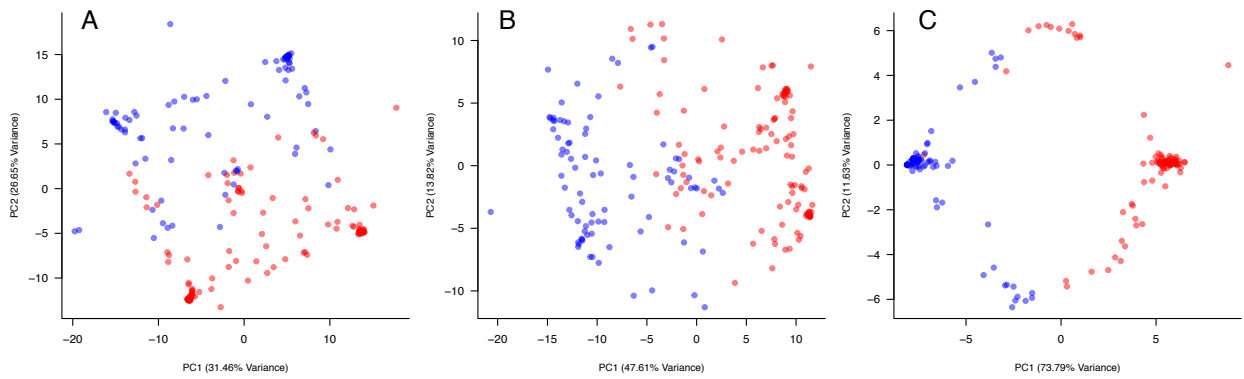


**Figure S16. Principal component analysis in the mating type region (MTR).** PCA of all *in vitro* and field isolates using the: A) 293 SNPs in the MTR; B) 184 significantly differentiated SNPs in the field F<sub>1</sub>; and the C) 51 SNPs significantly differentiated in both the field F<sub>1</sub> and inbred subpopulations.

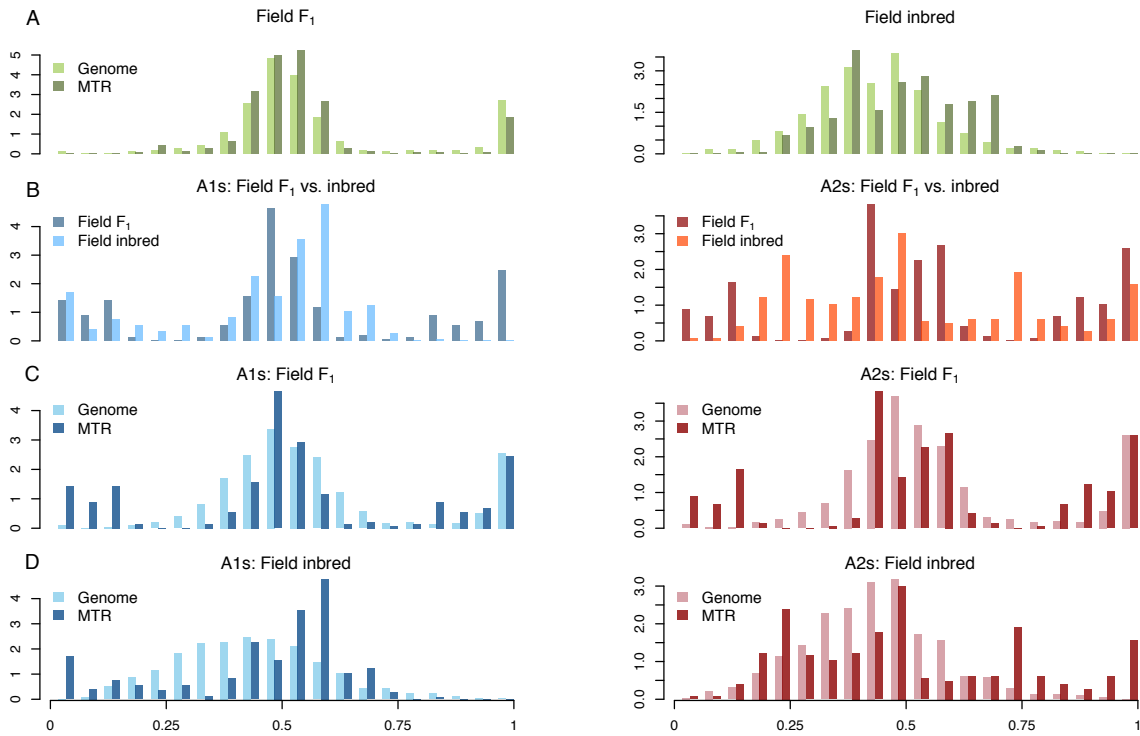


**Figure S17. Heterozygosity in the mating type region (MTR) compared to the rest of the genome.** Histograms of SNP heterozygosity in the MTR relative to the genome, represented by density distributions, for the: A) field F<sub>1</sub> and field inbred isolates; B) A1 and A2 field F<sub>1</sub> vs. field inbred isolates in the MTR; C) A1 and A2 field F<sub>1</sub> isolates in the MTR relative to the genome; and D) A1 and A2 field inbred isolates in the MTR relative to the genome.

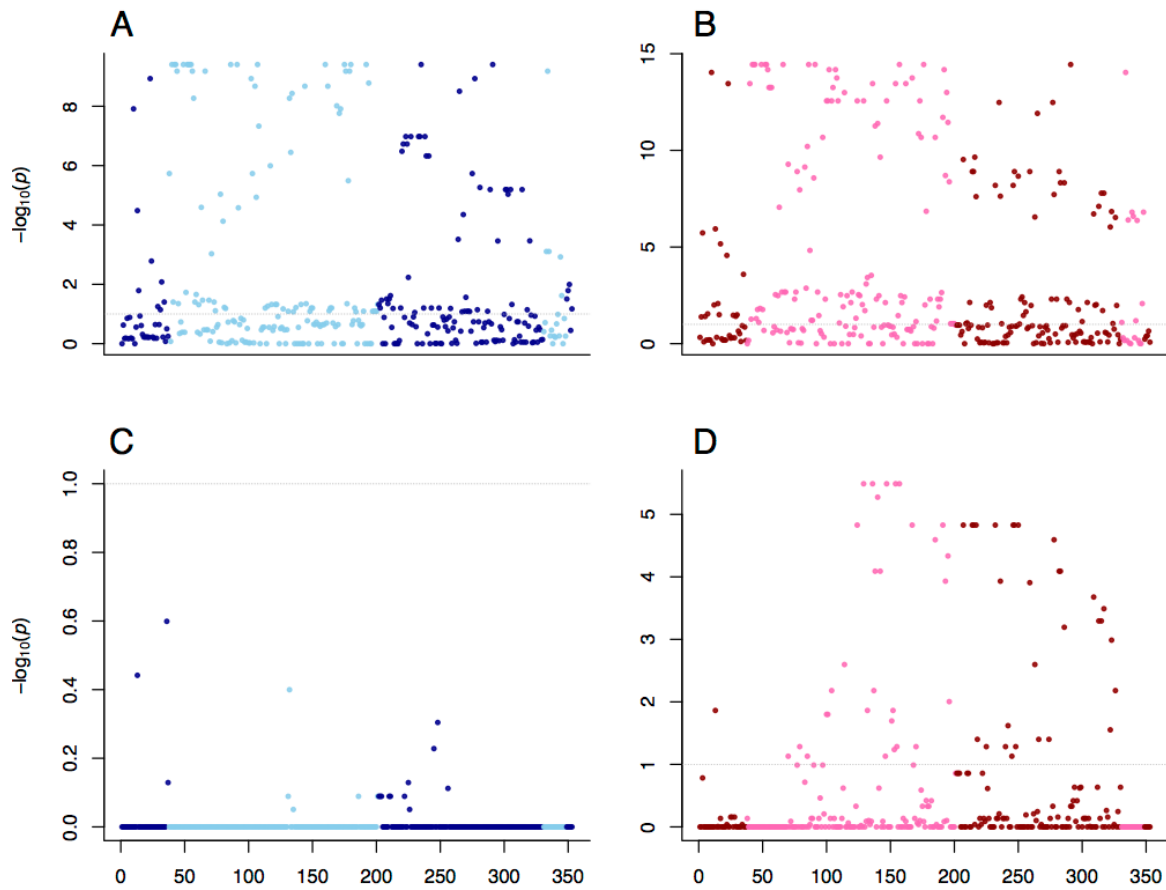


**Figure S18. Heterozygote excess in the mating type associated sub-regions.** Exact test of heterozygote excess in all five mating type associated sub-regions ( $n=353$  SNPs), ordered by scaffold (2, 4, 27, 34, and 40) and position within scaffold. For: A) A1 field  $F_1$  isolates; B) A2 field  $F_1$  isolates; C) A1 field inbred isolates; and D) A2 field inbred isolates.